Chemical Science

EDGE ARTICLE

View Article Online
View Journal | View Issue

Cite this: *Chem. Sci.*, 2017, **8**, 2290

Switchable slow relaxation of magnetization in the native low temperature phase of a cooperative spin-crossover compound†

A. Urtizberea and O. Roubeau*

Received 24th October 2016
Accepted 9th December 2016

DOI: 10.1039/c6sc04737h

www.rsc.org/chemicalscience

The implementation of single-molecule magnet properties in spin crossover materials is sought as a unique source of magnetic multistability at the molecular level. Examples however remain extremely scarce, in part due to the diamagnetic state of most Fe(II) spin crossover materials at low temperatures. We have studied the complex $[Fe(mtz)_6](CF_3SO_3)_2$ (mtz = 1-methyltetrazole) as a tantalizing candidate of such coexistence, due to its known partial spin crossover and therefore paramagnetic native low temperature phase. The single-crystal structures of $[Fe(mtz)_6](CF_3SO_3)_2$ reported here allow rationalizing its peculiar cooperative spin-crossover behavior. Importantly, the high-spin Fe crystallographic sites at low temperature exhibit a high symmetry with a local trigonal distortion, usually source of magnetic anisotropy. The analysis of equilibrium magnetic properties confirm the presence of a significant magnetic anisotropy at the Fe(II) high spin sites in the high symmetry low temperature phase. This results in field-induced slow relaxation of their magnetization which is dominated at low temperature by tunneling and direct processes and is strongly enhanced above 3 K by Raman and Orbach processes. Unprecedentedly, these single-molecule magnet properties are observed in the native ground state of a spin crossover material and efficiently and reversibly switched OFF through visible light irradiation.

Introduction

Magnetic bistability at the molecular scale is at the origin of exciting potential applications in molecular spintronics, quantum information processing or as sensors.[1] Arguably, the most relevant types of materials are those exhibiting Single Molecule Magnet (SMM) and spin crossover (SCO) behaviours. SMMs are characterized by the slow relaxation of their magnetization occurring thanks to the arising of an energy barrier to the molecular spin reversal that is related to a significant magnetic anisotropy.[2] Recent developments are mostly relying on mononuclear rare-earth[3] or transition metal[4] complexes designed to increase the molecular magnetic anisotropy, instead of the high-nuclearity strategy aimed at maximizing the spin ground state S.[5] In particular, great success has been obtained with low-coordinate or high symmetry environments in Fe[6] and Co[7] mononuclear complexes, both metals in addition potentially exhibiting a SCO process. Thermal SCO describes the reversible transition from a low spin (LS) ground state to a high spin (HS) state, made thermodynamically stable at high temperatures by its increased entropy.[8] It is naturally a single-ion phenomenon, although cooperative character giving rise to thermal bistability is the consequence of extended interactions in solids.[9] Here too, specific environments are required to yield the adequate ligand-field, a pseudo-octahedral N_6 donor for $3d^6$ Fe(II) ions, which represent the vast majority of SCO compounds. Their SCO involves an $S = 0$ diamagnetic LS state and an $S = 2$ HS state, that, in many cases, can further be reversibly interconverted through light irradiation.[10] Such an optically-controlled switch provided two of the few examples of light-activation of SMM properties, in the higher symmetry phase of the classic SCO compound $[Fe(ptz)_6](BF_4)_2$ (**1**, ptz = 1-propyltetrazole)[11] and in a four coordinate Fe(II) complex.[12] The combination of both SMM and SCO effects in one material, without requiring activation, is logically made difficult by the normally diamagnetic state of Fe(II) SCO materials at low temperatures and has indeed only been reported in one Fe(III) compound, with a 5-coordinate NP_2Cl_2 environment and SCO involving the intermediate 3/2 spin state as the ground LS state.[13] This peculiar system however did not provide the ability to switch the SMM properties OFF, but indicates that Fe(II) SCO materials with a partial SCO and therefore a paramagnetic phase at low temperature may be native SMMs with additional switching opportunities.

The coordination compound $[Fe(mtz)_6](CF_3SO_3)_2$ (**2**, mtz = 1-methyltetrazole) is known to exhibit a cooperative SCO of only 1/3 of its Fe(II) ions with a wide hysteresis, as demonstrated

Instituto de Ciencia de Materiales de Aragón (ICMA), CSIC and Universidad de Zaragoza, Plaza San Francisco s/n, 50009 Zaragoza, Spain. E-mail: roubeau@unizar.es

† Electronic supplementary information (ESI) available: CCDC 1493439 and 1493440. For ESI and crystallographic data in CIF or other electronic format see DOI: 10.1039/c6sc04737h

through Mössbauer spectroscopy and magnetic susceptibility.[14,15] The ability to transform the remaining HS Fe(II) ions to LS through light irradiation[14,15] remains one of the few cases of LIESST(H → L) (Light-Induced Excited Spin-State Trapping, HS to LS) effect.[10] These properties make compound **2** a tantalizing switchable SMM candidate, although no structural rationalization of its potential is possible as there has been so far no structure reported for **2**. Through an extensive calorimetric and structural study, we now have obtained a fully coherent picture of the phase diagram of this compound.‡ We report here the structures of the high and low temperature phases, the latter being of high symmetry and therefore relevant to the observation of SMM properties. The study of the dynamic magnetic properties of **2** then allows demonstrating it does exhibit unique switchable field-induced SMM properties. Our results represent the only example of coexistence of SCO and SMM in the stable ground state of a material, with the additional capacity to switch OFF/ON the SMM properties by light.

Results and discussion

Structural aspects

To understand the peculiar partial SCO of **2** and evaluate its potential SMM properties, knowledge of its crystal structure in its 1/3 LS phase at low temperatures and in the full HS phase appears fundamental. Single-crystals were obtained (i) directly by crystallization from the reaction mixture upon standing and (ii) by re-crystallization of a polycrystalline sample from nitromethane (ESI†). We found no difference in terms of magnetic and structural properties between the two methods.

At 200 K, compound **2** crystallizes in the triclinic $P\bar{1}$ space group (Table S1†) and is isostructural with its Ni analogue.[15] The cell content coincides with the formula, the unique Fe site sits on the inversion centre and the asymmetric unit thus has only three mtz ligands and one triflate anion (Fig. 1 top), disordered over two inverted positions. Fe–N bond lengths (avg. = 2.185(5) Å) are characteristic of an Fe(II) HS ion, in agreement with the magnetic properties (see below). N–Fe–N angles are in the range 88.75(7) to 91.25(7)° (Table S2†), the FeN_6 chromophore being close to an ideal octahedron (Table S2†). Indeed, the index Σ that measures the distortion of the first coordination sphere around the metal is only 11.6.[16] At 85 K, crystals of **2** are trigonal, crystallizing in the $R\bar{3}$ space group (Table S1†). The asymmetric unit has three distinct crystallographic Fe sites, all three on special positions with a 3-fold symmetry and 1/3 occupancy, three pairs of mtz ligands and two triflate anions, thus making for one formula unit, the cell containing 18 of these. One of the Fe sites, Fe1, has Fe–N bond lengths now depicting an Fe(II) ion in its LS state, *i.e.* 1.983(3) Å (N5) and 1.985(3) Å (N1) while the other two maintain longer Fe–N bond lengths typical of a HS state, respectively Fe2–N9 = 2.181(3) Å/Fe2–N13 = 2.183(3) Å and Fe3–N21 = 2.163(3) Å/Fe3–N17 = 2.221(3) Å. These structural observations fully explain the partial SCO of **2** detected in magnetic properties. As expected for a LS site, Fe1 is now closer to an ideal octahedron with $\Sigma = 9.1$, while Fe2 and Fe3 have similar and slightly larger Σ than in the 200 K structure, at respectively 12.1 and 21.6. Importantly and

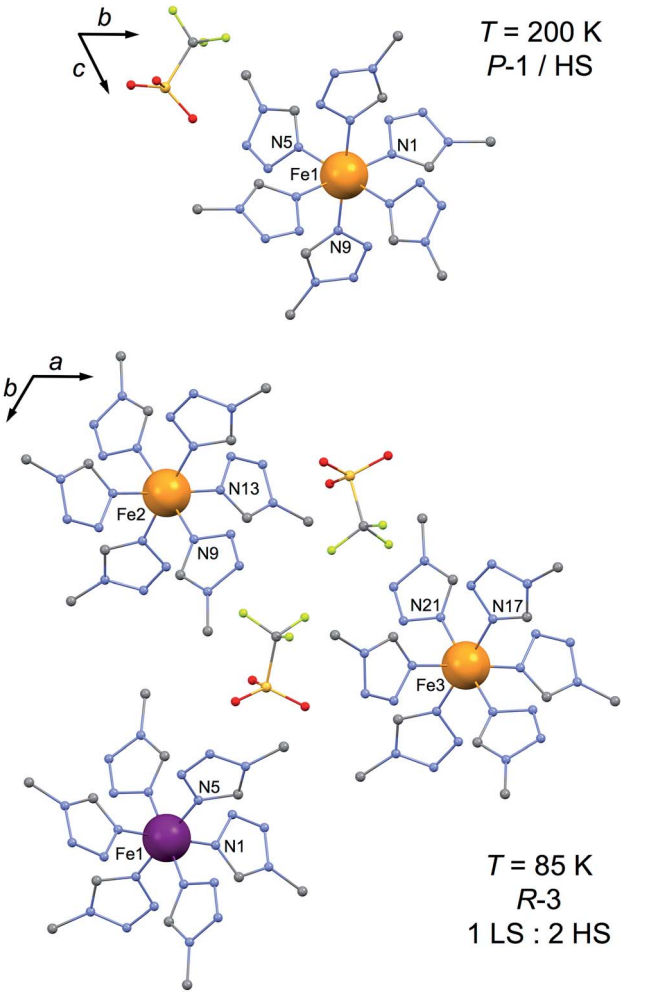

Fig. 1 Views of the structure of $[Fe(mtz)_6](CF_3SO_3)_2$ (**2**) in the HS triclinic phase at 200 K (top) and in the 1/3 LS rhombohedral phase at 85 K (bottom). For clarity, H are omitted and only the $CF_3SO_3^-$ anions pertaining to the asymmetric unit are shown, while full coordination environment of the Fe sites is depicted. Atomic sites involved in the coordination labelled. Colour code: Fe(II) HS, orange; Fe(II) LS, purple; S, light orange; F, yellow; O, red; N, light blue; C, grey.

due to the crystal symmetry, both Fe2 and Fe3 exhibit a D_{3d} local symmetry. This is relevant for the observation of SMM properties, since such a local distortion is at the origin of the SMM properties in the high symmetry light-induced HS phase of **1**,[11] even though only its cell parameters have been reported.[17]

The lattice packing and the involved intermolecular interactions remain very similar at both temperatures. In both structures, the $[Fe(mtz)_6]^{2+}$ cations form similar supramolecular hexagonal layers, reminiscent of analogue tetrazole complexes,[18,19] through C_{tz}–H···A hydrogen bonds with the triflate anions (Fig. 2, Table S3†). Weaker C_{Me}–H···A hydrogen bonds also involving the triflate ions connect these layers, with the shortest intermetallic separations in the range 7.21–7.92 Å (Fig. 2 and S1, Table S3†). The similarity of these intermolecular interactions with those found in the structures of other tetrazole compounds exhibiting gradual SCO[18a,19] suggests that the cooperative hysteretic SCO in **2** is associated with the presence of crystallographic transitions.‡

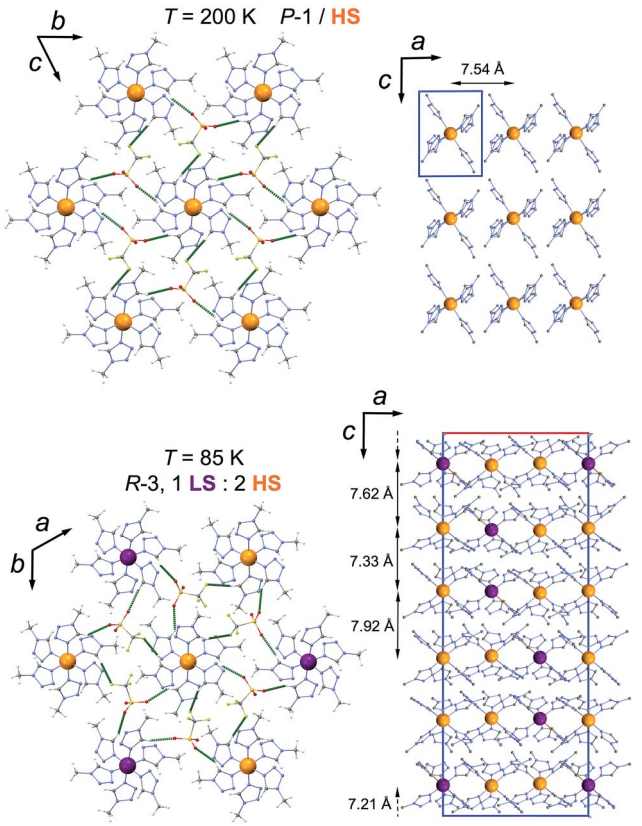

Fig. 2 Views of the structure of **2** at 200 K along the *a* (top left) and *b* (top right) axes and at 85 K along the *c* (bottom left) and *b* (bottom right) axes, showing respectively very similar layers of $[Fe(mtz)_6]^{2+}$ cations interconnected through the triflate anion by Ctz–H···A hydrogen bonds (green thick dashed lines, left), and the shortest Fe···Fe distances, corresponding to inter-layer separations (right). The unit cells are shown as thick blue and red lines. Colour code: large orange balls Fe(II) HS; large purple ball Fe(II) LS; small light blue balls, N; small grey balls, C; small white balls, H.

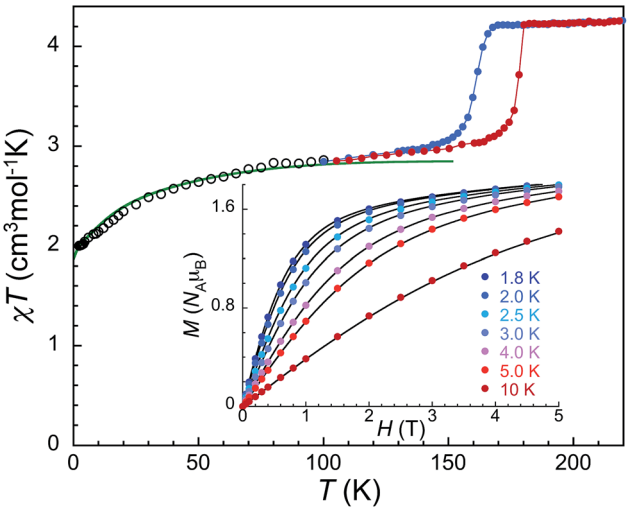

Fig. 3 Temperature dependence of the χT product as derived from dc measurements at 0.3 K min^{-1} and 0.5 T applied dc field (red/blue symbols respectively in cooling/warming mode) and zero-field ac measurements at 15 Hz (empty symbols). Inset: magnetization isotherms at the indicated temperatures. Green and black solid lines are the fit of the data to the model including spin–orbit coupling (see text).

Equilibrium magnetic properties

The existence of HS sites with local D_{3d} symmetry in the 85 K structure is compatible with the consideration that **2** may show SMM properties in its low temperature ground state. To evaluate this potential, we first re-examined the variable-temperature equilibrium magnetic properties of **2**.[20] An abrupt hysteretic SCO of 1/3 of the Fe(II) ions is observed in the χT *vs.* T plot (χ is the molar magnetic susceptibility, *i.e.* per Fe(II) ion), occurring at 178 and 161 K respectively upon warming and cooling (Fig. 3), in agreement with previous data,[14,15] and the 85 K structure. From the plateau at *ca.* 2.95 cm^3 mol^{-1} K below the SCO region, χT then exhibits a significant decrease from *ca.* 80 K, reaching 2.02 cm^3 mol^{-1} K at 2 K. This and the non-superposition on a single master curve of M *vs.* H/T plots (Fig. S2†) clearly indicate that the HS sites in **2** do present significant anisotropy.[21] To explain these magnetic properties the effective spin Hamiltonian $H = D[S_z^2 - 1/3S(S+1)] + E(S_x^2 - S_y^2) - \mu_B \cdot \boldsymbol{S} \cdot g \cdot \boldsymbol{H}$ is frequently employed, where g, D and E are the gyromagnetic tensor, here considered isotropic, and the axial and rhombic zero-field splitting (ZFS) parameters. A joint fit of χT *vs.* T and M *vs.* H data with PHI[22] gives $g = 2.42$, $D = -24.9$ cm^{-1} and $E = -1.1 \times 10^{-4}$ cm^{-1} (Fig. S3†). These parameters are in line with those obtained for the light-induced HS phase of **1** by EPR,[11] yet **2** shows slightly larger axial and smaller transverse anisotropies.

Noticeably, the magnitude χT at *ca.* 130 K, *i.e.* below the SCO temperature range, 2.95 cm^3 mol^{-1} K, is much larger than the expected spin-only value for 2/3 of Fe(II) $S = 2$ ion, 2 cm^3 mol^{-1} K (these translates to respectively 4.42 cm^3 mol^{-1} K and 3 if expressed per HS Fe(II) ion), resulting in the large g derived. Such large g values and the strong magnetic anisotropy have typically been assigned to orbitally degenerate Fe(II) possessing an unquenched orbital angular momentum,[21] which can be expected for Fe(II) in an Oh coordination with a cubic ligand field with slight trigonal distortion,[23] as observed in the structure of **2** at 85 K. A more realistic approach is thus to go beyond the spin Hamiltonian and instead, consider the presence of orbital angular momentum.[21] This involves the inclusion of spin–orbit coupling (SO), which can also be done using PHI.[22] The SO constant λ was left as fit parameter, and the crystal field parameterization was limited to the second order Stevens operators. The approach reproduces very well (Fig. 3 and S2†) the experimental data for $g = 2.09$, Stevens operators $B_2^0\theta_2 = -159.2$ cm^{-1}, $B_2^2\theta_2 = -1.2 \times 10^{-2}$ cm^{-1} and $\lambda = -100.0$ cm^{-1}. The energy schemes calculated using parameters obtained with both approaches parameters give energy gaps between the ground and first excited levels of 107.5 K (74.7 cm^{-1}) and 63.8 K (44.3 cm^{-1}), respectively. The latter model including SO is supported by the better agreement with M *vs.* H/T data (Fig. S2†), the indications of an orbital contribution in the magnitude of χT and the weak distortion to strict Oh environment,[23] observed for both HS crystallographic sites.

Importantly, the presence of orbital angular momentum often leads to stronger magnetic anisotropy than originating from ZFS, which is at the origin of synthetic design seeking unquenched angular momenta.[4,21] In any case, the derived anisotropy parameters suggest that the ground state of **2** is a good SMM candidate.

Dynamic magnetic properties

Examining the dynamic magnetic properties of **2**, no out-of-phase signal is detected in zero dc field at 1.9 K, but applying a small dc field does bring in such a frequency dependent component, indicative of slow relaxation of magnetization. This is characteristic of field-induced SMM behaviour, for which the applied field cancels out fast ground-state quantum tunnelling by breaking the $\pm m_S$ state degeneracy.[4] Frequency-dependent measurements in the range 1.9–5 K at optimal dc fields (1500 and 2000 Oe, see Fig. 4 left and S4 and S5†) confirm the SMM behaviour of **2**, and allow determining the temperature dependence of the spin–lattice relaxation time τ (Fig. 4 right, S6–S7†). The variation of τ with temperature at both fields is similar, dominated by a strong thermal activation above 3 K, and below longer relaxation times in the range 3–5 $\times$ 10^{-5} s with a weaker temperature variation. These data are satisfactorily reproduced by considering tunnelling, direct, Raman and Orbach components to the spin–lattice relaxation, $\tau^{-1} = R_{\text{tunnel}} + R_{\text{direct}}TH^2 + R_{\text{Raman}}T^5 + R_{\text{Orbach}}\Delta^3/[\exp(\Delta/T) - 1]$ (Fig. 4).[23] Tunnelling and direct processes dominate at lower temperatures ($R_{\text{direct}} = 1.9 \times 10^{-3}$ s^{-1} K^{-1} Oe^{-2}, $R_{\text{tunnel}} = 1.65 \times 10^4$ s^{-1} for 1500 Oe and 0.15 $\times$ 10^4 s^{-1} for 2000 Oe). At higher temperatures, Raman ($R_{\text{Raman}} =$ 72 s^{-1} K^{-5}) and Orbach ($\Delta = 55$ K, $R_{\text{Orbach}} = 9.7 \times 10^5$ s^{-1} K^{-3}) processes give rise to a strongly enhanced spin–lattice relaxation.

Interestingly, the energy of the excited state involved in the Orbach process, $\Delta = 55$ K (38.2 cm^{-1}), is in good agreement with the gap between ground and first excited levels determined from the equilibrium magnetic properties using the Hamiltonian including the unquenched angular momentum. Relaxation rates in **2** are about twice faster than those in the light-induced high-symmetry SMM phase of **1**.[11] This is likely related to a stronger distortion in the latter, although the lack of its structure impedes a detailed comparison. Most importantly, these observations support the strategy aiming at high symmetry 3d metal ions with a local axial distortion to obtain SMM.[4,6,7,12,21] Nevertheless, this is not straightforward at all for SCO materials. The fact the low symmetry light-induced HS phase of **1** does not exhibit SMM properties as opposed to its high-symmetry analogue[11] is along this line: not any light-induced HS phase or LT HS site of a SCO material will gather the conditions to behave as SMMs. In fact, it is rather the contrary, most will not. To highlight the importance of these considerations and the originality of **2**, we also studied the dynamic magnetic properties of $[Fe(mtz)_6](BF_4)_2$ (**3**). This analogue compound exhibits SCO of 1/2 of its Fe(II) centres, and therefore could be considered as a good SMM candidate given its chemical similarity with **2**. Nevertheless its low temperature phase is triclinic,[18a,24a] and therefore the LT HS site lacks the local trigonal distortion present for those in the structure of **2**. And indeed, the native LT HS phase of **3** does not exhibit any sign of slow relaxation of magnetization (Fig. S8†), in zero-field and up to 0.5 T applied dc field. Clearly, compound **2** is a very singular material that gathers unique conditions to observe SMM properties in the LT ground state of a SCO material, *i.e.* HS Fe(II) sites and local distortion giving rise to the required anisotropy. Both aspects are in fact separately already scarcely observed, and in particular there are only few SCO materials in which some of the crystallographic Fe(II) sites remain HS at low temperature.[24]

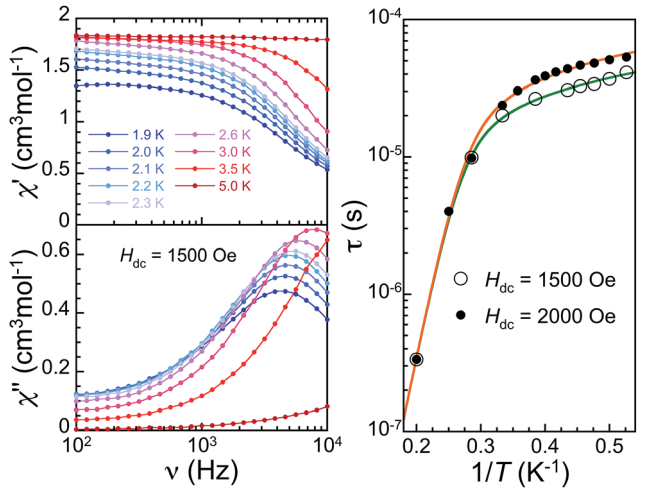

Fig. 4 Left: Frequency dependence of the in-phase (top) and out-of-phase (bottom) ac magnetic susceptibility of **2** under 1500 Oe dc field. Solid lines are guides for the eye. Right: Temperature dependence of the spin–lattice relaxation time τ at the indicated applied dc fields. Solid lines are fits to a model including tunnelling, direct, Raman, and Orbach relaxation processes (see text).

Reversible switching of SMM properties by irradiation

The transformation of the HS sites in compound **2** to their LS metastable state through the LIESST(H $\rightarrow$ L) effect has previously been observed through Mössbauer spectroscopy and magnetization measurements.[14,15] This should provide the means to switch OFF the observed SMM properties. However, incomplete transformations could only be obtained in both previous studies, respectively to *ca.* 73 and 87% LS.[14,15] This corresponds to steady-state situations resulting from the overlap of the $^5T_2 \rightarrow {}^5E$ band of the HS species with spin-forbidden bands of the formed LS species.[10,14,15] The larger residual HS fraction in the former study is likely the result of a too efficient irradiation in the broad and weak $^1A_1 \rightarrow {}^3T_2$ LS band at *ca.* 980 nm (Fig. S9†), by using light with $\lambda > 700$ nm of a Xe arc lamp, known to have strong intensities in the near infra-red. On the other hand, the latter study used broad-band irradiation of 700–800 nm, therefore of only a portion of the HS $^5T_2 \rightarrow {}^5E$ band. To reach a steady-state as close as possible to 100% LS, we used a thin sample and broad-band irradiation in the range 650–900 nm, therefore covering the most part of $^5T_2 \rightarrow {}^5E$ HS band while avoiding as much as possible irradiation in the $^1A_1 \rightarrow {}^3T_2$ LS band (Fig. S9†). Under these optimized conditions,

χT reaches values in the range 0.2–0.3 $cm^3\ mol^{-1}\ K$ within *ca.* 90 min (Fig. 5 left), indicating an efficient and almost complete conversion to LS. Conversely, the frequency-dependent ac susceptibility signal vanishes (Fig. 5 right), confirming the native SMM properties of **2** have been successfully switched OFF. Interestingly, the sample can be brought back to its original SMM phase through green-light irradiation (500–650 nm), the LIESST(L → H) effect being very efficient for the metastable LS sites Fe2 and Fe3 (complete within *ca.* 20 min, see Fig. 5 left), but ineffective at the native LS Fe1 site, in agreement with previous observations.[14,15] In addition, the process of switching OFF and ON is fully reproducible as indicated by repeated cycles.

It cannot be stressed enough that these original light-induced switchable SMM properties are the consequence of the unique character of compound **2** with respect to various key aspects. Indeed, **2** is one of the very few effective LIESST(H → L) cases occurring from a HS ground state, as opposed to from metastable HS species first trapped by LIESST(L → H). This is largely due to the fact that in most of these HS thermodynamically stable phases, the ligand field strength likely departs from those typical of SCO systems bringing the ^5E state below the intermediate ^3T state, thereby impeding the intersystem crossing to occur.[25] The fact we were able to reach a steady-state close to 100% LS is a further originality with respect to previous studies,[14,15] allowing a clean switching OFF of the SMM properties. Another important specificity of **2** is that the LIESST(L → H) does not take place at the Fe1 site, a very uncommon feature among Fe(II) SCO compounds.[10,26] This allows the switching of SMM properties to be fully reversible, since otherwise it would have been impossible to selectively transform only the Fe2 and Fe3 sites back to their original HS state. Altogether, these peculiarities make compound **2** the first native SMM SCO material with reversible photoswitching abilities.

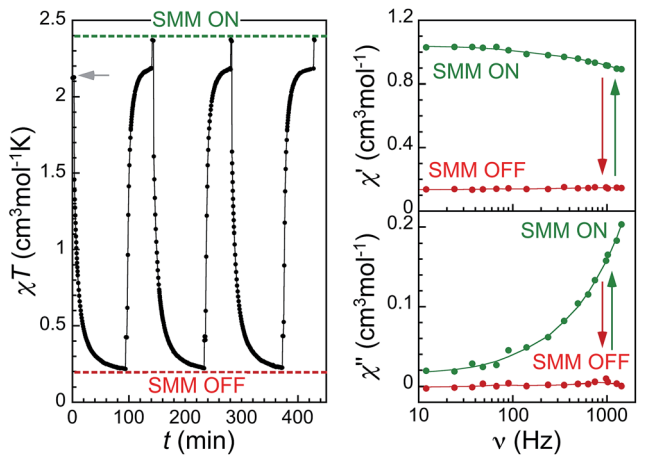

Fig. 5 Left: Time dependence of χT of a thin sample of **2** at 10 K and 0.5 T dc field showing three irradiation cycles with red (650–900 nm) and green (500–650 nm) light. Grey arrow indicates the χT value for a bulk sample of **2**. Right: Frequency dependence of the in-phase (top) and out-of-phase (bottom) ac magnetic susceptibility of **2** at 1.9 K under a 1500 Oe dc field. Solid lines are guides for the eye.

Conclusions

We have described the full HS high temperature and high-symmetry low temperature partial LS structures of the complex $[Fe(mtz)_6](CF_3SO_3)_2$. This allows to rationalize its peculiar cooperative SCO of only 1/3 of its Fe(II) centres and the significant magnetic anisotropy of the 2/3 HS ground state sites, associated with a local trigonal distortion. This anisotropy gives rise to single-molecule magnet properties in the compound native low-temperature phase, albeit only under an applied dc field. These properties can be efficiently and reversibly switched OFF and ON through red and green visible light, representing the first example of SMM properties in the native ground state of a SCO material and switchable through light. Our results support the validity of the approach aiming at tailoring SMM properties by the synthetic design of high symmetry 3d ions with a local axial distortion.

Acknowledgements

This work was supported by Spanish MINECO (projects MAT2014-53961-R and MAT2015-70868-ERC) and Aragón DGA (E-98 MOLCHIP). Structural data were collected at ALS beamline 11.3.1. The Advanced Light Source is supported by the Directors of the Office of Science and the Office of Basic Energy Sciences of the U. S. Department of Energy under contract no. DE-AC02-05CH11231.

Notes and references

‡ The full description of the complex dynamics and all structural phases present is beyond the scope of this report and will be published elsewhere.

1 (*a*) L. Bogani and W. Wernsdorfer, *Nat. Mater.*, 2008, **7**, 179; (*b*) R. Vincent, S. Klyatskaya, M. Ruben, W. Wernsdorfer and F. Balestro, *Nature*, 2012, **488**, 357; (*c*) G. Molnár, L. Salmon, W. Nicolazzi, F. Terki and A. Bousseksou, *J. Mater. Chem. C*, 2014, **2**, 1360.
2 D. Gatteschi and R. Sessoli, *Angew. Chem., Int. Ed.*, 2003, **42**, 268.
3 (*a*) N. Ishikawa, *Struct. Bonding*, 2010, **135**, 211; (*b*) J. Rinehart and J. R. Long, *Chem. Sci.*, 2011, **2**, 2078.
4 (*a*) G. A. Craig and M. Murrie, *Chem. Soc. Rev.*, 2015, **44**, 2135; (*b*) J. M. Frost, K. L. M. Harriman and M. Murugesu, *Chem. Sci.*, 2016, **7**, 2470.
5 G. Aromí and E. K. Brechin, *Struct. Bonding*, 2006, **122**, 67.
6 See for example: (*a*) D. E. Freedman, W. H. Harman, T. D. Harris, G. J. Long, C. J. Chang and J. R. Long, *J. Am. Chem. Soc.*, 2010, **132**, 1224; (*b*) J. M. Zadrozny, D. J. Xiao, M. Atanasov, G. J. Long, F. Grandjean, F. Neese and J. R. Long, *Nat. Chem.*, 2013, **5**, 577; (*c*) P. P. Samuel, K. C. Mondal, N. Amin Sk, H. W. Roesky, E. Carl, R. Neufeld, D. Stalke, S. Demeshko, F. Meyer, L. Ungur, L. F. Chibotaru, J. Christian, V. Ramachandran, J. van Tol and N. S. Dalal, *J. Am. Chem. Soc.*, 2014, **136**, 11964.
7 See for example: (*a*) S. Karasawa, G. Zhou, H. Morikawa and N. Koga, *J. Am. Chem. Soc.*, 2003, **125**, 13676; (*b*) F. Habib,

O. R. Luca, V. Vieru, M. Shiddiq, I. Korobkov, S. I. Gorelsky, M. K. Takase, L. F. Chibotaru, S. Hill, R. H. Crabtree and M. Murugesu, *Angew. Chem., Int. Ed.*, 2013, **52**, 11290; (*c*) J. M. Zadrozny, J. Telser and J. R. Long, *Polyhedron*, 2013, **64**, 209; (*d*) S. Gómez-Coca, A. Urtizberea, E. Cremades, P. J. Alonso, A. Camón, E. Ruiz and F. Luis, *Nat. Commun.*, 2014, **5**, 4300; (*e*) R. Díaz-Torres, M. Menelaou, O. Roubeau, A. Sorrenti, G. Brandariz-de-Pedro, E. C. Sañudo, S. J. Teat, J. Fraxedas, E. Ruiz and N. Aliaga-Alcalde, *Chem. Sci.*, 2016, **7**, 2793.

8 P. Gütlich and H. A. Goodwin, *Top. Curr. Chem.*, 2004, 233–235.

9 (*a*) B. Weber, W. Bauer and J. Obel, *Angew. Chem., Int. Ed.*, 2008, **47**, 10098; (*b*) O. Roubeau, *Chem.–Eur. J.*, 2012, **18**, 15230; (*c*) V. Niel, J. M. Martinez-Agudo, M. C. Muñoz, A. B. Gaspar and J. A. Real, *Inorg. Chem.*, 2001, **40**, 3838.

10 A. Hauser, *Top. Curr. Chem.*, 2004, **234**, 155.

11 X. Feng, C. Mathonière, I.-R. Jeon, M. Rouzières, A. Ozarowski, M. L. Aubrey, M. I. Gonzalez, R. Clérac and J. R. Long, *J. Am. Chem. Soc.*, 2013, **135**, 15880.

12 C. Mathonière, H.-J. Lin, D. Siretanu, R. Clérac and J. M. Smith, *J. Am. Chem. Soc.*, 2013, **135**, 19083.

13 S. Mossin, B. L. Tran, D. Adhikari, M. Pink, F. W. Heinemann, J. Sutter, R. K. Szilagyi, K. Meyer and D. J. Mindiola, *J. Am. Chem. Soc.*, 2012, **134**, 13651.

14 P. Gütlich and P. Poganiuch, *Angew. Chem., Int. Ed. Engl.*, 1991, **30**, 975.

15 A. F. Stassen, O. Roubeau, I. Ferrero Gramage, J. Linarès, F. Varret, I. Mutikainen, U. Turpeinen, J. G. Haasnoot and J. Reedijk, *Polyhedron*, 2001, **20**, 1699.

16 Σ is sum of the deviations of the twelve *cis* N–Fe–N bite angles from 90°, see P. Guionneau, M. Marchivie, G. Bravic, J. F. Létard and D. Chasseau, *Top. Curr. Chem.*, 2004, **234**, 97.

17 J. Kusz, H. Spiering and P. Gütlich, *J. Appl. Crystallogr.*, 2000, **33**, 201.

18 (*a*) L. Weihl, *Acta Crystallogr., Sect. B: Struct. Sci.*, 1993, **49**, 289; (*b*) J. Kusz, M. Zubko, R. B. Neder and P. Gütlich, *Acta Crystallogr., Sect. B: Struct. Sci.*, 2012, **68**, 40.

19 (*a*) G. Aromí, L. A. Barrios, O. Roubeau and P. Gamez, *Coord. Chem. Rev.*, 2011, **255**, 485; (*b*) O. Roubeau, E. Natividad and M. Evangelisti, *Chem. Commun.*, 2012, **48**, 7604.

20 Probable orientation effects, avoided here by restraining the polycrystalline sample in grease, were ascribed to a ferromagnetic interaction in ref. 15.

21 (*a*) P. H. Lin, N. C. Smythe, S. I. Gorelsky, S. Maguire, N. J. Henson, I. Korobkov, B. L. Scott, J. C. Gordon, R. T. Baker and M. Murugesu, *J. Am. Chem. Soc.*, 2011, **133**, 15806; (*b*) A. V. Palii, J. M. Clemente-Juan, E. Coronado, S. I. Klokishner, S. M. Ostrovsky and O. S. Reu, *Inorg. Chem.*, 2010, **49**, 8073; (*c*) S. Gómez-Coca, E. Cremades, N. Aliaga-Alcalde and E. Ruiz, *J. Am. Chem. Soc.*, 2013, **135**, 7010.

22 N. F. Chilton, R. P. Anderson, L. D. Turner, A. Soncini and K. S. Murray, *J. Comput. Chem.*, 2013, **34**, 1164.

23 A. Abragam and B. Bleaney, *Electron Paramagnetic Resonance of Transition Ions*, Dover, New York, 1986.

24 In mononuclear complexes: (*a*) P. Poganiuch, S. Decurtins and P. Gütlich, *J. Am. Chem. Soc.*, 1990, **112**, 3270; (*b*) R. Hinek, H. Spiering, D. Schollmeyer, P. Gütlich and A. Hauser, *Chem.–Eur. J.*, 1996, **2**, 1427; (*c*) J. A. Kitchen, G. N. L. Jameson, J. L. Tallon and S. Brooker, *Chem. Commun.*, 2010, **46**, 3200; In dinuclear complexes: (*d*) M. H. Klingele, B. Moubaraki, J. D. Cashion, K. S. Murray and S. Brooker, *Chem. Commun.*, 2005, 987.

25 A. Hauser, *Coord. Chem. Rev.*, 1991, **111**, 275.

26 In fact all $Fe^{II}N_6$ tetrazole complexes studied so far exhibit LIESST(L → H), except compound **2**.